

# Journal of Photonics for Energy

PhotonicsforEnergy.SPIEDigitalLibrary.org

## **Laser processing for thin film chalcogenide photovoltaics: a review and prospectus**

Brian J. Simonds  
Helene J. Meadows  
Sudhajit Misra  
Christos Ferekides  
Phillip J. Dale  
Michael A. Scarpulla

# Laser processing for thin film chalcogenide photovoltaics: a review and prospectus

Brian J. Simonds,<sup>a</sup> Helene J. Meadows,<sup>b</sup> Sudhajit Misra,<sup>c</sup>  
Christos Ferekides,<sup>d</sup> Phillip J. Dale,<sup>b</sup> and Michael A. Scarpulla<sup>a,c,\*</sup>

<sup>a</sup>University of Utah, Electrical and Computer Engineering, Salt Lake City,  
Utah 84112, United States

<sup>b</sup>University of Luxembourg, Physics and Materials Research Unit, Belvaux L4422, Luxembourg

<sup>c</sup>University of Utah, Materials Science and Engineering, Salt Lake City, Utah 84112,  
United States

<sup>d</sup>University of South Florida, Electrical Engineering, Tampa, Florida 33620, United States

**Abstract.** We review prior and on-going works in using laser annealing (LA) techniques in the development of chalcogenide-based [CdTe and Cu(In, Ga)(S, Se)<sub>2</sub>] solar cells. LA can achieve unique processing regimes as the wavelength and pulse duration can be chosen to selectively heat particular layers of a thin film solar cell or even particular regions within a single layer. Pulsed LA, in particular, can achieve non-steady-state conditions that allow for stoichiometry control by preferential evaporation, which has been utilized in CdTe solar cells to create Ohmic back contacts. Pulsed lasers have also been used with Cu(In, Ga)(S, Se)<sub>2</sub> to improve device performance by surface-defect annealing as well as bulk deep-defect annealing. Continuous-wave LA shows promise for use as a replacement for furnace annealing as it almost instantaneously supplies heat to the absorbing film without wasting time or energy to bring the much thicker substrate to temperature. Optimizing and utilizing such a technology would allow production lines to increase throughput and thus manufacturing capacity. Lasers have also been used to create potentially low-cost chalcogenide thin films from precursors, which is also reviewed. © The Authors. Published by SPIE under a Creative Commons Attribution 3.0 Unported License. Distribution or reproduction of this work in whole or in part requires full attribution of the original publication, including its DOI. [DOI: [10.1117/1.JPE.5.050999](https://doi.org/10.1117/1.JPE.5.050999)]

**Keywords:** thin film photovoltaics; laser processing; CdTe; CIGS; annealing.

Paper 14080 received Oct. 15, 2014; accepted for publication Dec. 8, 2014; published online Jan. 19, 2015.

## 1 Introduction

Lasers are appealing for use in semiconductor manufacturing as they are capable of high throughput and precise operations. The majority of the research and implementation of lasers for solar cell production has been directed toward crystalline silicon solar cells where lasers have been used for edge isolation,<sup>1,2</sup> hole drilling for emitter and metal wrap-through cells,<sup>3</sup> surface texturing for light trapping,<sup>4</sup> firing contacts,<sup>5,6</sup> etc. These applications have recently been reviewed in the literature.<sup>7,8</sup> In thin film photovoltaics (PV), lasers have been used for the recrystallization of amorphous Si into polycrystalline Si<sup>9,10</sup> and scribing for the monolithic cell integration of CdTe<sup>11</sup> and Cu(In, Ga)(S, Se)<sub>2</sub> (CIGS)<sup>11,12</sup> cells. The aim of this paper is to review laser-based processes for synthesizing and or improving the properties of the chalcogenide absorber layers used in thin film solar cells, namely CdTe and Cu(In, Ga)S(Se). Such processes have the potential to both increase solar cell efficiency and reduce manufacturing costs in ways unachievable by standard thermal processing. We begin by discussing general aspects of laser annealing (LA) independent of the material type. Then, we review doping, back contact formation, and grain growth for CdTe. In the last section, synthesis of Cu(In, Ga)Se<sub>2</sub> from

\*Address all correspondence to: Michael A. Scarpulla, E-mail: [scarpulla@eng.utah.edu](mailto:scarpulla@eng.utah.edu)

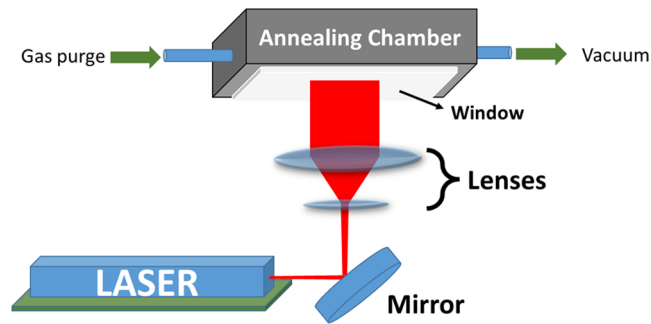


**Fig. 1** A general schematic of a laser annealing (LA) apparatus.

precursor material is reported as well as efforts to reduce defect densities in the semiconductor using lasers.

A typical schematic of a laboratory scale LA apparatus is shown in Fig. 1. This relatively simple setup allows for a wide range of experimental conditions. The samples to be treated can be placed in a gas-tight chamber to control the annealing environment. This chamber can be mounted on a motion stage to allow for scanning of the sample in the beam line. For large-scale manufacturing necessary for PV, scanning of the annealing beam would be more desirable as moving an entire solar panel beneath the beam would be prohibitively difficult. Beam scanning can be accomplished by combinations of galvomirrors and f-theta lenses to direct the beam while maintaining beam quality. Additional lenses can be used to change the size and shape of the annealing beam to obtain the necessary power densities. For instance, cylindrical lenses can be used to create a collimated line beam ideal for scanning larger areas.

Recent developments in laser technology have made lasers available at a wide range of wavelengths, pulse durations and output powers for a reasonable cost. Lasers are, therefore, appealing for replacing traditional furnace-based processes in order to reduce capital expenditures. Laser processing, in particular, continuous wave (CW) LA can have several advantages over furnace processing or even rapid thermal processing (RTP). Lasers provide a local source of heat as only the absorbing layer(s) of a cell are directly heated. Therefore, a several microns thick thin film will heat almost instantaneously to start the annealing kinetics without waiting for the entirety of the typically several millimeters thick substrate to reach equilibrium in a furnace. This also means that the temperature threshold of the substrate will no longer be the limiting criterion for solar cell processing. As an example, polyimide substrates have been investigated to replace glass for making flexible, thin film solar cells.<sup>13,14</sup> However, its lower critical temperature of about 400°C becomes the upper limit that any film can be processed at if furnaces are used, which would not necessarily be the case with laser processing. In addition, by judicious selection of laser wavelength, specific layers of the thin film stack can be targeted.

Figure 2 shows the bandgap wavelengths for several common semiconductors used for thin film PV along with the output wavelength of several commercially available lasers. For example, a Ti:Sapphire laser line operating at 800 nm could target the  $\text{Cu}_2\text{ZnSnS}_4$  (CZTS) absorber layer while not directly being absorbed in the CdS emitter layer of a CZTS-based solar cell. This again allows for a wider range of processing conditions.

The temperature reached during LA strongly depends on the strength of the absorption at the wavelength used and the laser beam dwell time. Similar temperatures can be reached under a variety of different experimental conditions, which is reflected by a wide range of experimental LA conditions used in the literature. For instance, a strongly absorbed light rapidly scanned at high laser intensity can produce similar temperatures as a longer dwell time with lower intensity. The preferred condition will largely be determined by the kinetics of the desired material process being elicited by the laser. The thermal properties of the film(s) and substrates also play a large role in determining the peak temperature with large temperature gradients occurring during LA that are not present during furnace annealing where isothermal conditions are assumed. Therefore, calculations of temperatures achieved during LA can be extremely useful in determining the appropriate laser parameters for a particular experiment. Although laser parameters can be optimized based on empirical findings, temperature modeling based on optical and thermal properties of the materials can also be used to guide experimentation and interpret results.<sup>15-17</sup>

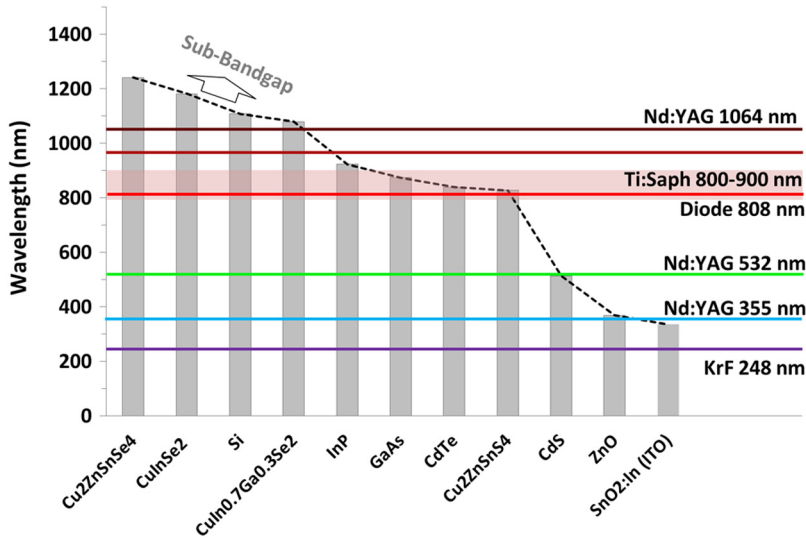


**Fig. 2** A comparison of the wavelength corresponding to the bandgap of common semiconductors used for thin film solar cells along with the lasing wavelengths of several different lasers.

Pulsed laser annealing (PLA) is uniquely suited to affecting surface regions by utilizing short laser pulses at wavelengths that are absorbed very near the film surface. The laser-induced kinetics are largely limited near the surface since thermally activated processes, like diffusion and evaporation, will be dominated at the light-incident surface due to the presence of steep temperature gradients.<sup>18</sup> The heat-affected zone (HAZ) during PLA is the larger of either the penetration depth,  $d$ , at the wavelength used or the thermal diffusion length,  $l_t$  defined by<sup>19</sup>

$$l_t = \sqrt{2Dt}, \tag{1}$$

where  $D$  is the thermal diffusivity and  $t$  is the pulse duration. The penetration depth is the inverse of the absorption coefficient or  $1/\alpha$ . To illustrate this, Fig. 3 shows  $l_t$  versus a range of pulse

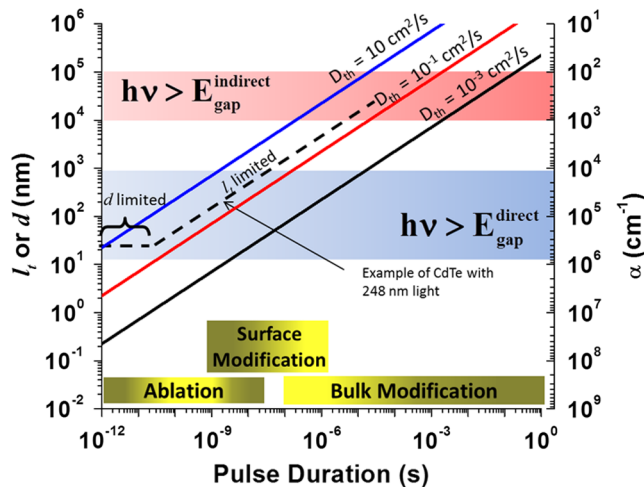


**Fig. 3** The plot of the thermal diffusion length,  $l_t$ , versus pulse duration as defined by Eq. (1) for different values of thermal diffusivity (solid lines) compared to the penetration depth,  $d$ . The corresponding values of absorption coefficient are given on the right axis with the shaded regions signifying the range for common direct and indirect bandgap solar cell materials. An example of CdTe illuminated with 248-nm pulsed radiation is shown with the dashed curve where the regions of penetration depth and thermal diffusion limited behavior are labeled. Along the bottom axis are indicated typical pulse durations for different laser induced processes. The darker shading indicates the most common time regimes.

widths for different values of  $D$ . Also shown are typical regions of  $\alpha$  for direct and indirect semiconductors ( $E_{\text{gap}}^{\text{direct}}$  and  $E_{\text{gap}}^{\text{indirect}}$ ) with their corresponding  $d$  values on the left axis.

As an example, the dashed line in Fig. 3 shows the situation where a KrF excimer pulse at 248 nm (5.0 eV) is incident to CdTe. At this wavelength  $d \approx 30$  nm ( $\alpha = 3 \times 10^5 \text{ cm}^{-1}$ ) and  $D = 0.055 \text{ cm}^2 \text{ s}^{-1}$  for polycrystalline CdTe.<sup>20</sup> From the figure, it is clear that at pulse durations longer than about 30 ps, the HAZ will be determined by  $l_t$  where longer pulses mean deeper heat penetration. Only for pulses shorter than  $\sim 30$  ps will the optical absorption determine the HAZ depth. For reference, along the bottom of Fig. 3 are shown the typical time scales of different laser processes used in PV manufacturing or research. Ablation refers to any process where material is removed as in scribing, hole drilling, or pulsed laser deposition. Surface and bulk modification time scales are also shown and these are the main subjects of this review. Specific experimental conditions for particular references are stated explicitly below.

## 2 Laser Processing of CdTe

Polycrystalline CdTe is a leading thin film PV technology due to its near ideal bandgap ( $\approx 1.5$  eV) for sunlight absorption and its high absorption coefficient as it is a direct bandgap semiconductor. In addition, it was the first photovoltaic technology to break the  $\$1/W_p$  cost barrier (in 2009) and is currently at or below  $\$0.59/W_p$ .<sup>21</sup> Recent advances have seen a dramatic increase in the record efficiency for single junction CdTe devices, which had remained dormant around 17% for about two decades. In the past 2 years, however, the record efficiency has catapulted to 21%.<sup>22</sup> This is notable as it not only shows that large improvements are possible in relatively short timescales, but also puts CdTe on par with the other major thin film technology, Cu(In, Ga)Se<sub>2</sub> (21.7%),<sup>23</sup> as well as multicrystalline silicon.<sup>24</sup> Although these improvements are promising for CdTe PV, the record is still considerably lower than its theoretical limit, near 30%. Therefore, continued research in device structure and operation are imperative.

Laser processing offers unique opportunities to address technological issues affecting CdTe device efficiencies as well as lowering manufacturing costs by increasing module throughput. Past research of the laser processing of CdTe can be grouped by those processes that affect a narrow surface region and those that affect the bulk, which are depicted in Fig. 4. Surface processing [Fig. 4(a)] typically uses pulsed lasers with photon energies that are several times higher than the bandgap ( $E_{\text{gap}} \approx 1.5$  eV = 827 nm) and are thus strongly absorbed near the surface. For example, a KrF excimer laser at 248 nm (5.0 eV), which has a penetration depth of 30 nm in CdTe, is commonly used for surface modification. The pulse energy can be used to change the surface stoichiometry through preferential evaporation and alter surface morphologies. Laser processing of the bulk [Fig. 4(b)] is performed with deeper penetrating light (energy near, but lower than  $E_{\text{gap}}$ ), which is typically CW. In this regime, lasers are used for film recrystallization and defect annealing.

### 2.1 Laser-Induced Surface Modification

The leading CdTe solar cells are based on a superstrate design (glass/TCO/CdS/CdTe/back contact), where the CdTe absorber is the final layer deposited before back contact metallization with the light impinging through the glass substrate. Ohmic contacts are vital in solar cells as they allow for the maximum collection of photogenerated carriers. The formation of an Ohmic contact in the final metallization step has long been a difficult task due to CdTe's high electron affinity and its propensity to form surface dipoles that pin the Fermi level.<sup>25</sup> As a result of these dipoles, even very large work function metals do not necessarily make an Ohmic junction.<sup>26</sup> A non-Ohmic contact in a solar cell behaves essentially as a reverse polarity Schottky diode and results in a second depletion width in the cell leading to poor fill factor and losses in open-circuit voltage ( $V_{\text{oc}}$ ) and short-circuit current ( $J_{\text{sc}}$ ),<sup>27</sup> all of which lower the device's efficiency. Several engineering techniques have been devised to create quasi-Ohmic contacts including the addition of highly doped p-type buffer layers, preferential chemical etches, or combinations of both. A heavily p-doped surface region between lightly p-type CdTe and metal will create an Ohmic junction by allowing hole flow through a narrowed tunneling region. Recently, PLA has been

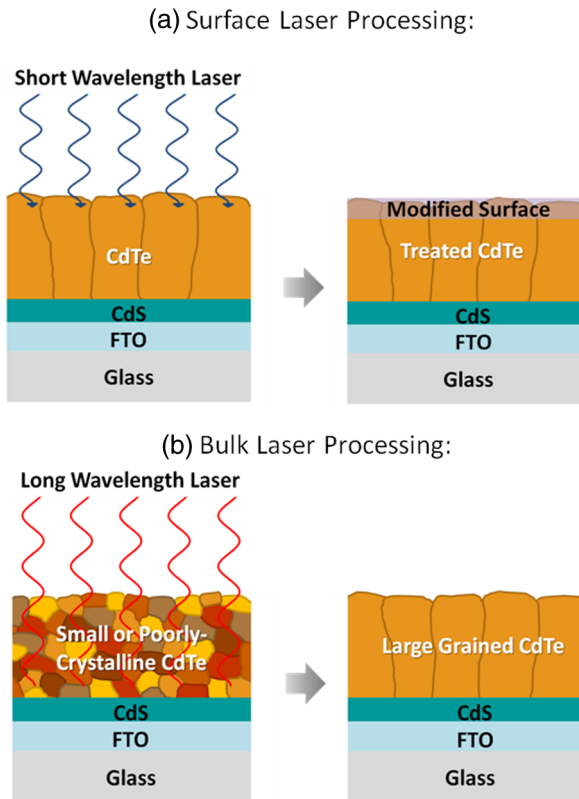


**Fig. 4** The two ways in which lasers have been used for polycrystalline CdTe processing: (a) surface modification and (b) bulk recrystallization and defect annealing.

used for creating an Ohmic back contact.<sup>28,29</sup> A pulsed laser-based approach has several advantages including not requiring additional vacuum processing, being highly tunable through pulse number and fluence, and it does not create a Cd-contaminated liquid waste stream as is the case with chemical etches.

An Ohmic back contact is created with PLA by exploiting the difference in vapor pressure between Cd and Te, with Cd being the more volatile species.<sup>30,31</sup> When a pulsed UV laser is applied, the surface rapidly heats to very high temperatures causing slightly more Cd loss than Te. This can leave either a Te-rich surface, which effectively dopes the surface highly p-type due to the increased presence of Cd vacancy acceptors, or leaves a thin Te film, or some combination of both.<sup>32</sup> Elemental Te is a degenerate p-type semiconductor and thin layers on the surface of CdTe have been shown to lead to Ohmic behavior,<sup>33</sup> although this may be due more to the formation of metal tellurides than to the properties of Te itself, as has been discussed.<sup>34</sup> Pulsed laser-induced stoichiometry changes were first noted, albeit casually, by Montgomery et al. as they investigated the use of 400 ns pulses of 590 nm light to prepare clean crystalline CdTe surfaces.<sup>35</sup> Brewer et al. more fully explored the phenomenon using a KrF excimer laser with 15 ns pulses and showed that above a threshold fluence, a Te-rich surface was created before the onset of melting.<sup>31</sup> Furthermore, it was discovered that this behavior was completely reversible by the application of sub-threshold light, which suggested to the authors that the mechanisms responsible were a temperature-related competition between Cd and Te<sub>2</sub> desorption. A Te surface enrichment with ruby or KrF laser pulses has been experimentally confirmed by several other groups.<sup>36–38</sup> Golovan et al. calculated the surface temperature reached during PLA by accounting for the heat losses due to evaporation of Cd and Te.<sup>39</sup> This was later adapted by us for use in a three-dimensional finite-element model of laser interactions with CdTe.<sup>18</sup>

Pulsed laser-induced surface modification was first applied to the more PV-relevant polycrystalline CdTe by Nelson et al. by annealing 200 to 300 nm thick CdTe films using 8 ns pulses of the second, third and fourth harmonic of a Nd:YAG laser.<sup>40</sup> They performed x-ray photoemission microscopy to show that a Te-rich surface was produced. These films were highly idealized

as they were grown in ultra-high vacuum and had a much larger grain size to film thickness ratio ( $>1 \mu\text{m}$ : 200 to 300 nm) than is typical of PV device-quality CdTe. Simonds et al. showed that PLA using a KrF excimer laser of thin film CdTe was capable of making an Ohmic back contact in CdTe PV devices by applying laser pulses before back contact metallization.<sup>28</sup> Transfer length measurements showed that a single, 25-ns pulse was capable of lowering the specific contact resistivity by a factor of over 20. Current-voltage measurements of completed devices revealed that after 100 pulses, all signs of a non-Ohmic back contact had disappeared. Further investigations of the surface chemistry induced by PLA suggested that the Te-layer was not uniform but concentrated at the exposed surfaces at grain boundaries,<sup>32</sup> which was also noted previously.<sup>40</sup> Although it is clear that a PLA is capable of much more rapidly producing an Ohmic back contact, further work is necessary to show how the device performance compares with other established techniques of creating Ohmic contacts. This is an ongoing topic of our research.

During standard deposition processes of thin film CdTe for PV, it is empirically well-known that CdTe congruently sublimes, meaning stoichiometric films are readily attained. However, the above literature shows that with PLA, this is not the case. In fact, even CW illumination has been seen to cause incongruent sublimation of Cd and Te.<sup>15,41–45</sup> This was demonstrated by Soares et al. using micro-Raman spectroscopy, where a distinct spectral line from elemental Te was seen to grow as a result of increasing intensity of the Raman excitation laser source.<sup>44,45</sup> An example of this phenomenon is shown in Fig. 5 from our own micro-Raman measurements where an as-deposited polycrystalline CdTe sample is continuously exposed to the excitation light with spectra taken every 5 min. One sees that a spectral line ( $A_1$ ) due to an optical mode of elemental Te<sup>46</sup> near  $120 \text{ cm}^{-1}$  grows as a result of CW exposure to the excitation source. Soares et al. were able to calculate the surface temperature by comparing the intensity ratios of the Stokes and anti-Stokes Raman signals and found that in their measurement, the surface was  $\sim 200^\circ\text{C}$  above room temperature, which is well below the melting threshold of  $1092^\circ\text{C}$  for CdTe.<sup>45</sup> A careful measurement of the crater depth versus temperature created by CW illumination is compared to that expected by purely thermal sublimation of Cd and  $\text{Te}_2$  by Uzan et al., who revealed that the activation energy of the laser induced process was 1.44 eV smaller than the assumed thermal process.<sup>15</sup> The fact that this value is nearly identical to the bandgap of CdTe (especially at elevated temperature) suggests that a recombination-induced athermal mechanism is responsible for Cd vacancy,  $V_{\text{Cd}}$ , and creation. Furthermore, Tsyutsura and Shkumbatyuk showed that it was possible to use CW  $\text{CO}_2$  laser light to create a shallow p-n junction in indium-doped n-type

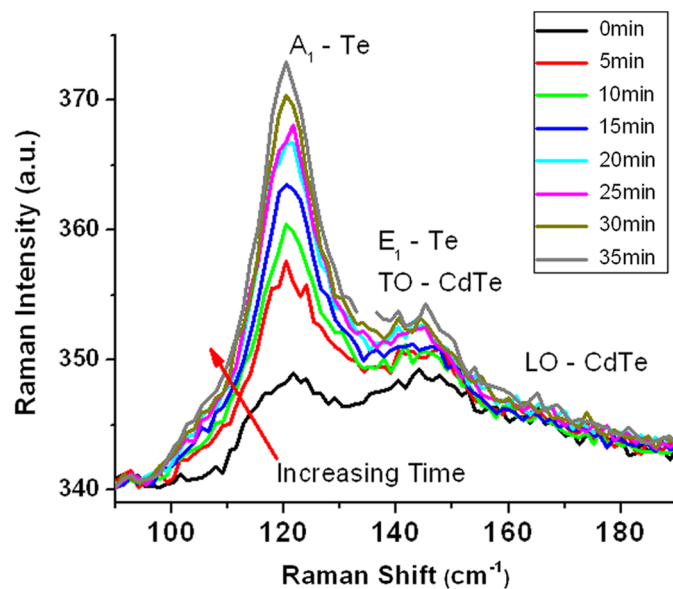


**Fig. 5** Micro-Raman measurements at 5-min intervals while being continuously exposed to the 532-nm CW excitation source. The peak near  $120 \text{ cm}^{-1}$  is due to elemental Te ( $A_1$ ). The broad peak at  $145 \text{ cm}^{-1}$  is an overlap of a Te peak ( $E_1$ ) and a transverse optical (TO) mode of CdTe. The low intensity shoulder near  $165 \text{ cm}^{-1}$  is due to CdTe.

crystalline CdTe.<sup>47</sup> They claimed that the junction formation was due to a laser-induced redistribution of n-type  $V_{Cd}$ - $In_{Cd}$  complexes into  $In$  interstitials and  $V_{Cd}$  acceptors. In light of this evidence, it seems most likely that additional  $V_{Cd}$  were also being produced during CW LA thereby being at least partially responsible for the creation of the p-type region. These hypotheses have not been completely explored but have shown that LA allows for processing conditions that are not possible by traditional thermal means.

## 2.2 Laser Processing for Bulk Effects in CdTe

Recombination of photoexcited carriers by deep-defects results in very short minority carrier lifetimes and low open-circuit voltages and is, therefore, a major culprit in limiting the performance of CdTe devices.<sup>48</sup> Additionally, the deposition of high quality polycrystalline CdTe is currently one of the slowest steps in completing a solar cell module and requires process parallelization in order to maintain the total average cycle time of the other, much faster, module production processes.<sup>49</sup> Therefore, a method of rapidly depositing CdTe, even if initially lower in quality, followed by a rapid LA process to increase grain size and anneal defects could potentially save on capital costs and increase module throughput. In this section, we will review evidence from literature which shows that LA is capable of achieving both of these material effects.

First, as a proof-of-principle that LA can be used to rapidly improve initially low-quality material, Fig. 6 shows x-ray diffraction (XRD) data before and after CW 1064 nm LA for 100 s of sputtered CdTe made without substrate heating during deposition. Although the laser photon energy (1.17 eV) is below the nominal bandgap of CdTe, appreciable heat is generated due to direct absorption by defect states.<sup>17</sup> Four distinct peaks are seen: (100), (101), and (002) from a wurtzite phase<sup>50</sup> and the {111} zincblende phase with the latter two overlapping. The presence of a local wurtzite crystal structure is synonymous with stacking faults which result in poor electrical quality.<sup>51</sup> Figure 6 clearly shows the ability of LA to reduce the presence of the wurtzite phase and the extended defects associated with it: the wurtzite peaks decrease in intensity and the zincblende peaks become narrower upon LA.

The LA of polycrystalline CdTe was first studied by Dawar et al., who used a ns-pulsed 1064 nm Nd:YAG laser on 700 nm CdTe.<sup>52</sup> By increasing the pulse energy and number, they showed that grain growth from 45 to 103 nm could be achieved, as well as a more than doubling of the mobility. They also measured, via Hall measurements, an increase in the carrier activation energy that they attributed to defect creation, which increased with pulse fluence and number. This is perhaps a result of stress introduced during PLA and is possibly why subsequent studies have relied on CW laser anneals. Indeed, our own initial findings with PLA of defective CdTe

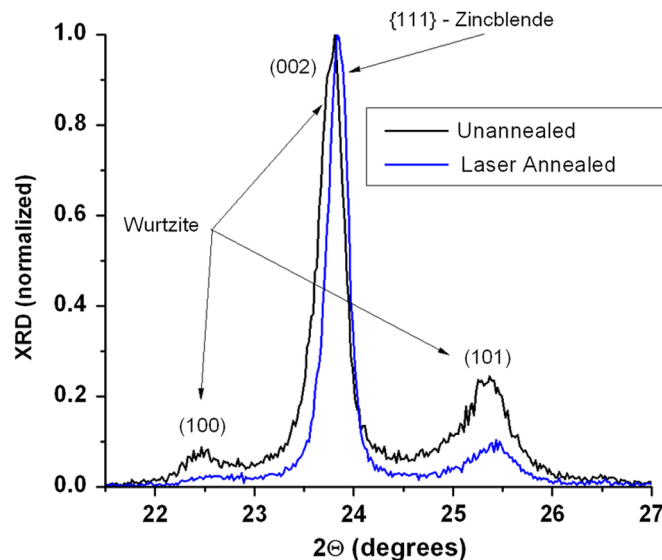


**Fig. 6** XRD data of as-deposited, low quality CdTe that was laser annealed with CW 1064 nm light with 100 s dwell time.

showed grain growth, but increased levels of strain are not shown. Grain growth has also been seen with CW LA with an 808-nm light source rapidly scanned across the film surface.<sup>53</sup>

Laser recrystallization of large-grained epitaxially grown films has also been shown to quickly increase grain size. As and Palmetshofer<sup>54</sup> showed that the maximum grain size increased after only 2 s exposure of CdTe:In films to 647-nm CW light. Defect concentrations were compared between laser annealed and isochronal thermal annealed samples with photoluminescence (PL) and deep-level transient spectroscopy. These measurements revealed that the laser and thermal annealing mechanisms are fundamentally different in that deep defects, not seen after LA, but appear after thermal annealing at comparable temperatures. Other LA studies of epitaxial CdTe showed that LA was capable of relieving microstresses in the films as well as decreasing surface roughness.<sup>55</sup> LA has also been investigated to repair radiation-induced damage,<sup>56–59</sup> where in some cases, it has been found to be more effective than furnace annealing.<sup>57,59</sup> For instance, Schuller et al. found that a 2-s CW LA gave similar lattice repair to radiation damaged CdTe as a 15 min isothermal furnace annealing.<sup>59</sup>

Recently, our group has shown that sub-bandgap CW light (1064 nm, Nd:YAG) can improve the optical and crystalline quality of initially low-grade polycrystalline CdTe.<sup>17</sup> The absorption in these films is due to defect states, which were shown to be reduced upon LA. This was monitored *in situ* by measuring the partially transmitted laser light during the annealing. This work has not only shown the ability of LA to rapidly improve material quality, but also revealed a new technique by which real-time process control can be implemented to improve throughput.

Several novel methods of using lasers to rapidly crystallize precursor films into thin film CdTe have been studied. Baufey et al. deposited alternating layers of Cd and Te and employed pulsed and CW laser light to synthesize and crystallize thin film CdTe.<sup>60</sup> They found that the LA parameters can be varied to successfully obtain PV-relevant zincblende phase CdTe with 500-nm sized grains. The CW annealing gave larger grain sizes that were single zincblende phase, whereas the PLA resulted in a mixed phase that included wurtzite crystal structure. Electrophoresis using polar organic solvents followed by LA has also been explored as a low-cost deposition route and has achieved deposition rates of 20  $\mu\text{m}/\text{min}$ .<sup>61</sup> A rapidly scanned (0.2 to 0.6 mm/s) argon laser line (514 nm) produced the highest quality films when compared to furnace or PLA with a 1064 nm light. They also found that the presence of CdCl<sub>2</sub> was vital for enhancing recrystallization. Additionally, pulsed UV lasers have been used to photodissociate organometallic precursors to create epitaxial CdTe thin films.<sup>62,63</sup> However, the very slow deposition rates on the order of 1  $\mu\text{m}/\text{h}$  will ultimately limit the usefulness of this technique for PV applications.

A more promising route for using LA to rapidly produce thin film CdTe from a low-cost precursor is from the sintering of CdTe nanoparticles that can readily and cheaply be chemically synthesized. Rickey et al. employed a novel technique of pulsed-laser induced compression followed by PLA.<sup>64</sup> Several hundred MPa of compression were first applied to nanoparticle films by an unspecified “highly absorbing material” in intimate contact with the nanoparticle mesh that was rapidly expanded by the absorption of a 5 ns, 1064 nm laser pulse. The compressing material was then removed and two 7.05 mJ, 25 ns pulses (wavelength not specified) were applied to the compressed film. It was found that these two pulses were sufficient to sinter the particles and achieve film resistances similar to those found in conventional polycrystalline CdTe. Unfortunately, no optoelectronic characterization was undertaken and the films were far from optimal. However, this or related techniques seem to warrant further investigation for low-cost PV applications.

### 3 Laser Processing of Cu(In,Ga)Se<sub>2</sub>

CuInSe<sub>2</sub> (CISe) and the solid state alloy Cu(In,Ga)Se<sub>2</sub> (CIGSe) have shown prominence as absorber layers in PV devices reaching recorded power conversion efficiencies of  $\geq 21\%$ .<sup>23</sup> (Subsequently, the term CI(G)Se will be used when referring to either CISe or CIGSe.) There are two primary routes used to form these chalcopyrite absorber layers: (1) vacuum co-evaporation to deposit and crystallize the constituent elements in a single step and (2) deposition of a precursor film followed by high temperature annealing and selenization to transform the precursor into a single phase, highly crystalline layer, suitable for use in devices. The

precursor film is normally deposited either by a vacuum technique such as sputtering or an ambient temperature and pressure method like electrodeposition. Annealing is carried out either using a furnace or RTP oven over timescales ranging from a few minutes to 2 h.<sup>65,66</sup>

Two key approaches have been pursued for LA of CI(G)Se, as illustrated in Fig. 7. CW LA [Fig. 7(a)] uses dwell times of milliseconds or longer to stimulate long-range atomic diffusion, grain growth, and chemical reactions. Figure 7(b) shows PLA that fires high energy nanosecond pulses with rapid repetition rates to provide bursts of energy typically localized near the film surface. The short, high energy bursts increase atomic mobility within this region due to a rapid temperature increase and are, therefore, able to modify defect levels and increase crystalline ordering at the surface of a CI(G)Se film. Operated in the non-melt regime, it is possible to only induce a short-range increase in crystalline ordering but is insufficient for notable grain growth. High enough laser intensities using either PLA or CW annealing will melt the CI(G)Se film and lead to much higher atomic mobilities and greater opportunity for crystal growth than solid state processing. However, the liquefied absorber should not dewet the substrate as this would lead to pinholes in the solidified absorber layer and subsequent electrical shunting in the full device. Examples can be found in the literature of the dewetting of the liquid film and non-crystalline or nanocrystalline solidification induced by the rapid cooling of the liquid.<sup>67,68</sup>

Due to the fundamental differences between PLA and CW LA, each has a very different objective when applied to CI(G)Se. CW LA aims to replace the furnace or RTP step in the above mentioned method (2), transforming a chemically inhomogeneous precursor into a crystalline CI(G)Se absorber with suitable properties to be completed into a device. On the other hand, PLA is a supplemental technique used to enhance the optoelectronic properties of a fully formed CI(G)Se absorber layer, however it has been formed. We can make this differentiation between the capabilities of CW and PLA because we have fully explored the processing parameter space and have demonstrated that there is no processing window in the ns or faster regime in which a precursor can be converted to an absorber layer within a shorter time than traditional annealing without the deleterious melting of the sample.<sup>68</sup> In this section, the research and results achieved using each of these techniques are examined.

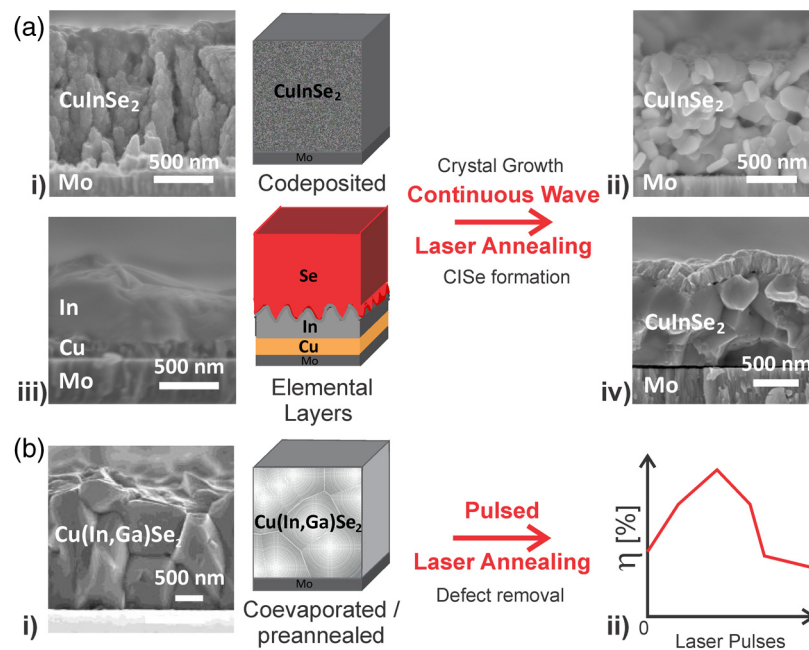


**Fig. 7** Representation of the two different approaches to LA  $\text{Cu}(\text{In}, \text{Ga})\text{Se}_2$ . (a) Continuous-wave LA showing schematics and cross sectional SEM micrographs of (i) co-deposited  $\text{CuInSe}_2$  precursor and (ii) after LA with 1064 nm Nd:YAG laser (1 s dwell time), and elemental layers of Cu/In/Se (iii) precursor and (iv) after laser anneal with 1064 nm Nd:YAG laser for  $\approx 2$  s and etched in 5% KCN for 60 s. (b) Pulsed laser annealing (PLA) with (i) SEM cross sectional micrograph of a co-evaporated  $\text{Cu}(\text{In}, \text{Ga})\text{Se}_2$  precursor and a schematic of the effect of LA on efficiency.

### 3.1 CW Laser Annealing

Figures 7a(i) and 7a(iii) depict the two precursor types that have been used for CW LA. The annealing objectives in both cases are to fully homogenize the elements and promote Cu(In, Ga)Se<sub>2</sub> grain growth. The first precursor, shown in Figure 7a(i), consists of the constituent elements deposited by electrodeposition in a single step at room temperature to form a nanocrystalline film. While the nanocrystallinity leads to high excess grain boundary energy, there is only a minimal chemical driving force to change the precursor since the precursor consists of binary and ternary selenides. By contrast, the metallic elements, Cu, In, and Se, can also be deposited in separate steps to form a stack, as shown in Fig. 7a(iii). This second precursor type has a much greater requirement for atomic diffusion and chemical reaction than the co-deposited precursor, but is chemically much more reactive since the elements have an oxidation state of zero. In order to stimulate the transformation processes of atomic diffusion, grain growth and chemical reaction, the LA must supply sufficient energy. Below, the approaches are described which have, to date, been used to achieve this aim.

#### 3.1.1 Annealing of Cu/In/Se stacks

In 1985, Joliet and Laude published the first research on LA of CISE.<sup>68,69</sup> They chose the most chemically reactive CISE precursor: stacked elemental layers (SELs) of Cu/In/Se, as shown in Fig. 7a(iii). A CW Ar<sup>+</sup> laser ( $\lambda = 457.9$  to  $514.5$  nm),  $0.7$  s “pulse” (mechanically chopped laser irradiation) and fluxes  $100$  to  $650$  W cm<sup>-2</sup> on free standing (without substrate), SEL precursors of  $100$  nm total thickness, led to single-phase CuInSe<sub>2</sub> with crystal sizes of up to  $20$   $\mu$ m. An alternative CW rastering process was also demonstrated by these authors<sup>68,69</sup> for similar precursor stacks mounted on glass substrates. A dwell time of  $0.5$  s per unit area and fluxes of  $200$  to  $500$  W cm<sup>-2</sup> resulted in the formation of a single-phase CISE absorber but with smaller grains in the range of  $0.1$  to  $1$   $\mu$ m, as measured by transmission electron microscopy. The grain size in both films was dependent on the power density. The difference in final crystallite size between the two methods is explained by localized melting occurring in the free standing films during annealing, where the absence of a substrate prevents thermal conductance away from the film. Bhattacharyya et al.<sup>70</sup> extended this approach, keeping the same laser wavelength and dwell times but increasing the precursor thickness to  $1.5$   $\mu$ m, which is suitable for photovoltaic devices.<sup>71</sup> Even with an increased film thickness and lower fluxes ( $<100$  W cm<sup>-2</sup>) than in the CW experiments of Laude and Joliet,<sup>68,69</sup> a similar  $0.5$  to  $1$   $\mu$ m grain size was measured in the final absorber.<sup>71</sup> At fluxes  $>80$  W cm<sup>-2</sup>, the film was single phase. However, at power densities below this threshold, there existed secondary phases, which included binary selenides (e.g., CuSe, In<sub>2</sub>Se<sub>3</sub>) and metallic compounds (CuIn). Based on these observations, a reaction scheme was proposed for the formation of CISE from SELs by LA that proceeds via the binary selenides similar to that proposed and observed for furnace annealing. This contradicts Laude et al.<sup>68</sup> who proposed a near-instantaneous (on the order of  $10^{-9}$  s), direct interatomic coupling reaction, facilitated by a liquid In-Se layer over the Se and the nanometer-scale film thickness. The peak temperature in the irradiated SEL precursor was postulated by Laude and modeled by Bhattacharyya to reach between  $900^{\circ}\text{C}$  and  $1100^{\circ}\text{C}$ ,<sup>70</sup> which is sufficient to melt the In and Se layers and promote rapid reactions. However, these temperatures also exceed the vaporization temperature of Se,  $T_{\text{vap}}: \text{Se} = 685^{\circ}\text{C}$ ,<sup>72</sup> leading to Se loss, and are potentially above the melting temperature of CISE ( $990^{\circ}\text{C}$ ).<sup>73</sup> Sub-stoichiometric amounts of Se lead to absorber layers with poor opto-electronic performance and which have melted, as discussed above.<sup>73</sup> Melted CISE dewets from the Mo substrate forming micrometer droplets.<sup>70</sup>

In an effort to further reduce LA time, Walter et al.<sup>74</sup> increased the reactivity of their SEL precursors by depositing the precursor as nine layers (i.e., three stacks of Cu/(In or Ga)/Se). This creates a high interfacial potential energy within the precursor and using powers in the range of  $1$  kW cm<sup>-2</sup>, reduced annealing dwell times to tens of milliseconds. This result demonstrates the huge potential for process time reduction realizable using LA in the synthesis of CI(G)Se absorbers. However, to date, no device characteristics have been demonstrated for this method and, therefore, its true value as a synthesis route for CI(G)Se thin film solar cells cannot be evaluated. As outlined above, there are two issues that are hypothesized to limit the progress of this method. First,

dewetting of the film<sup>70</sup> leads to a morphology incompatible with substrate configuration thin film solar cells due to direct connection between the front contacts and Mo back contact. Second, the volatility of elemental Se means that it is easily lost from the sample at the calculated laser processing temperatures. Without a method to ensure this, Se remains available to the stack so that the formation of a CI(G)Se semiconductor with any reasonable optoelectronic properties is impossible.

In order for the LA of Cu/In/Se precursors to be taken seriously, it is now necessary to show that such annealed films also have suitable optoelectronic properties, ideally demonstrated in working devices. In the next section, we will review CW LA of CISE co-deposited precursors and show that they can have suitable optoelectronic properties as well as form working devices.

### 3.1.2 Annealing of co-deposited Cu-In-Se

Subsequent approaches to the CW LA of CISE have focused on co-deposited Cu-In-Se films [see Fig. 7a(i)], where stoichiometric quantities of each of the constituent elements are deposited in a single step. This process distributes Se evenly through the film depth and the majority is bound to Cu and/or In atoms as opposed to existing in its free state. Jost et al.<sup>75</sup> initiated this processing route by using a Nd:YAG ( $\lambda = 1064$  nm) to anneal co-electrodeposited CISE films. Comparing the results of samples annealed at incident laser fluxes from 11.6 to 36.8 kW cm<sup>-2</sup> to those that had been annealed in a furnace for 5 min at 550°C, the LA absorbers demonstrated higher crystallinity (as determined from the narrowing of CISE Bragg-peaks in XRD diffractograms). This result was achieved by subjecting the film to rapid thermal cycling achieved by scanning the 110  $\mu$ m beam at 100 mm s<sup>-1</sup> 20 times. This gave a total annealing time of 22 ms, which is four orders of magnitude faster than “rapid” annealing processes. However, as with the rapid annealing of SELs in the previous section, the CISE film was seen in SEM micrographs to dewet the substrate.

Consequently, our work on CW annealing of CISE focuses on solid state processing. This was initially achieved by a significant drop in laser flux to 0.05 kW cm<sup>-2</sup> to avoid melting, with typical anneal times between 15 and 60 s.<sup>67</sup> The SEM of such CISE films’ surfaces showed no change in their surface appearance with LA, consistent with a non-melt process. Analyzing the bulk of the material using XRD showed that LA increased the crystalline order determined by a narrowing of the characteristic chalcopyrite peaks in the x-ray diffractogram. The effect of metal composition on the crystallinity was tested by annealing “Cu-rich” (Cu/In > 1) and “Cu-poor” (Cu/In < 1) precursors. The CISE crystal structure is tolerant to a wide range of stoichiometries<sup>76</sup> and the adjustment of this parameter remains an interesting research topic.<sup>77</sup> While record CISE devices have a Cu-poor final composition,<sup>78</sup> they often include a Cu-rich growth step that is observed to enhance optoelectronic and structural properties.<sup>79</sup> Our group<sup>67</sup> also measured a narrower 112 XRD peak for laser annealed absorbers from Cu-rich precursors when compared to their Cu-poor counterparts. Mooney and Hermann<sup>80</sup> revealed that the extinction coefficient,  $k$ , which describes the attenuation of electromagnetic radiation by a material, is dependent on stoichiometry and ranged from 0.15 for Cu-poor to 0.3 for Cu-rich electrodeposited precursors. A higher  $k$  leads to a higher power density being dissipated in the absorber, as demonstrated in the calculations of Ref. 67, which used a transfer matrix approach to analyze power absorption versus depth. The increased energy absorbed by Cu-rich films results in higher peak film temperatures during LA, and a faster rate of atomic diffusion, grain growth and defect removal than the Cu-poor samples. So, both higher optical absorption and greater atomic mobility are related to Cu richness and probably combined to result in the observed differences versus precursor film Cu composition.

Initial work by our group established a 15 s minimum annealing time to yield structural improvements in electrodeposited CISE films.<sup>67,81</sup> Although 15 s is faster than a 5-min RTP process<sup>75</sup> or up to 60-min furnace process,<sup>82</sup> it neither demonstrates the full potential of this rapid heating technique nor offers a significant energy savings over current industrial furnace processing. Furthermore, shorter annealing times, particularly when achieved with a technique compatible with roll-to-roll processing, can dramatically increase industrial throughput. Consequently, further work has focused on an “intermediate” time/flux regime.<sup>83–86</sup> Fluxes between 150 and 945 W cm<sup>-2</sup> and a dwell time up to 1 s gave a noticeable structural improvement. This is measurable as an observed increase in grain size between precursor and annealed

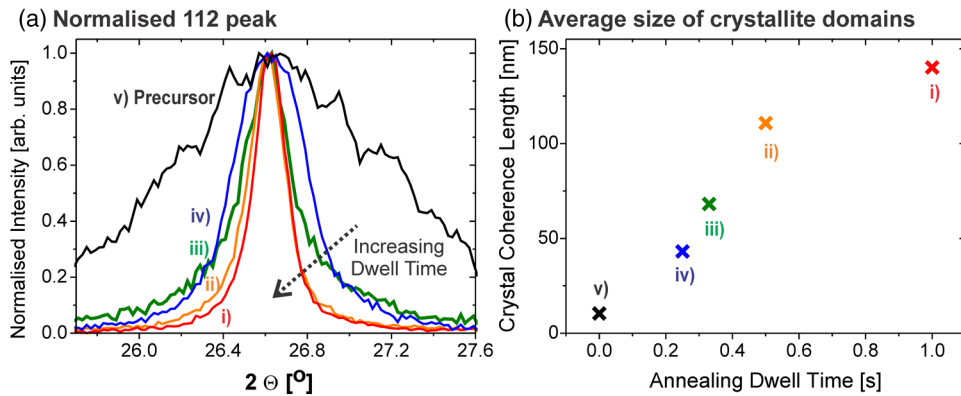


**Fig. 8** (a) XRD diffractograms ( $\theta - 2\theta$ ) of  $\text{CuInSe}_2$  absorbers focusing on 112 peak, after LA Cu-In-Se precursors with Nd:YAG laser at  $150 \text{ W cm}^{-2}$ , with scan speeds (corresponding to annealing times) of (i)  $2 \text{ mm s}^{-1}$  (1 s), (ii)  $4 \text{ mm s}^{-1}$  (0.5 s), (iii)  $6 \text{ mm s}^{-1}$  (0.3 s), (iv)  $8 \text{ mm s}^{-1}$  (0.25 s), (beam area:  $2 \times 2 \text{ mm}^2$ ), compared to (v) precursor. (b) Crystallite coherence lengths of determined from FWHM of 112 peak of the diffractograms of (a).

samples in SEM [see Figs. 7a(i) and 7a(ii)] and the CISE peaks in the XRD diffractogram become narrower with a longer annealing time [illustrated in Fig. 8(a)]. Calculating the crystal coherence length from these peaks using the Scherrer equation shows apparent average crystallite domain sizes of 43 to 140 nm for 0.25 to 1 s dwell time [Fig. 8(b)]. The 140-nm crystallite domain size achieved with 1-s dwell time, and  $150 \text{ W cm}^{-2}$  is larger than that achieved for  $50 \text{ W cm}^{-2}$  for 15 to 60 s.<sup>67</sup> Hence, crystallite domain size growth is a function of both flux and time, and as will be seen below, also depends on the selenium vapor pressure above the sample.

Importantly, this work was the first to test the optoelectronic properties of an absorber formed by LA, which indicated an increase in photoelectrochemical photocurrent and a higher level of radiative recombination as compared to the precursor. However, the initial device efficiency from an absorber formed in this process was negligible. An XRD study,<sup>84</sup> evidenced that these absorbers may contain an unreacted  $\text{In}_2\text{Se}_3$  secondary phase, and/or structural defects, quenched by the rapid cooling following laser irradiation. The cause for the low efficiency, however, was believed to stem from the loss of volatile Se from the film, even within the 1-s annealing time.<sup>83</sup> Se may be lost directly from the Se lattice resulting in  $\text{V}_{\text{Se}}$  defects, which have been correlated to poor device performance,<sup>87</sup> or resulting from the decomposition of the CISE semiconductor into its binary selenides.

In order to prevent Se loss, subsequent LA experiments were carried out under a background partial pressure of Se.<sup>85,86,88</sup> A higher Se activity led to an increased  $\text{Se}/(\text{Cu} + \text{In})$  ratio in the absorber, as well as larger grains and a higher PL yield as compared to lower Se activity.<sup>86</sup> Figure 9(a) illustrates the difference in the PL yield of absorbers annealed under high and low partial pressures of Se. Implementing this new approach, the first and only known working solar cell device to date with a LA absorber was fabricated with a power conversion efficiency of 1.6%.<sup>88</sup> Characteristic patterns on the surface of this absorber [Fig. 8(b)] appear to be linked to the rastering of the  $2 \times 2 \text{ mm}^2$  laser beam over the surface. The Gaussian spatial profile of the power distribution was shown to affect the annealing temperature profile of the CISE film.<sup>85</sup> This uneven energy distribution stimulates different levels of grain growth and atomic diffusion perpendicular to the beam scanning direction, and consequently, variations in lateral optoelectronic properties are expected. As is well known, fluctuations in properties for solar cells result in voltage and efficiency loss; essentially, the cell performance is linked to the lowest quality material in the device. It is believed that with a homogeneous beam flux, and minimal thermal variance over the sample area, a consistent photon conversion would be achieved over the full device area, and higher power conversion efficiencies would be achieved.

LA of co-deposited precursors shows that it is possible to stimulate sufficient atomic diffusion, chemical reaction, grain growth, and enhancement of optoelectronic properties with  $\leq 1$  s dwell time while remaining in the solid state regime. This process has enabled the first device to be fabricated where transformation from CISE precursor to absorber was achieved using only a

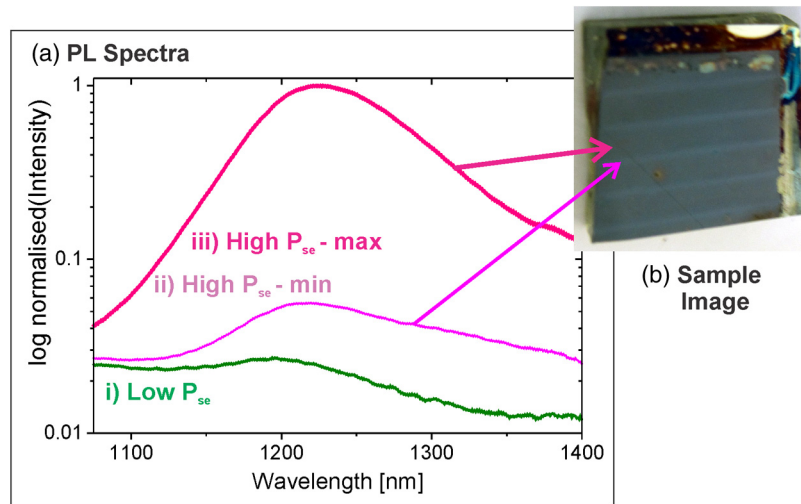


**Fig. 9** (a) PL Spectra of  $\text{CuInSe}_2$  co-deposited precursor and after annealing at  $150 \text{ W cm}^{-2}$ , 1 s dwell time per unit area, with (ii) a low  $P_{\text{Se}}$  ( $\approx 9 \times 10^{-7} \text{ Pa}$ ), and (iii) a higher  $P_{\text{Se}}$  ( $\approx 2 \times 10^{-4} \text{ Pa}$ ). These areas correlate, respectively, to the pale and dark lines observed on the absorber surface as indicated in (b).<sup>88</sup>

laser. Although the efficiency of this device is low, key points for improvement are identified, which include homogenizing the laser beam flux and increasing the background Se activity during annealing. This provides opportunity for future work to increase device efficiency and consequently allow this processing route to compete with current methods.

### 3.2 Pulsed Laser Annealing

An alternative LA process tested on  $\text{CI(G)Se}$  is PLA. This differs substantially in both the material and annealing objectives as compared with CW LA. CW annealing gives a constant power output, whereas PLA is characterized by high peak power but a much lower average power. The energy supplied during the very short pulses will rapidly heat the film. However, the pulse times remain below those required for thermal equilibrium, leading to large temperature gradients. PLA initially found favor in removing damage caused by ion-implantation in the near-surface regions of Si wafers.<sup>89</sup> PLA of  $\text{CI(G)Se}$  aims to modify defects and thus enhances final device efficiency. All reported studies of PLA in  $\text{CI(G)Se}$  use a 248-nm excimer laser (pulse width,  $w \approx 25 \text{ ns}$ ), which has a penetration depth of 50 nm in  $\text{CISE}$  and a heat affected region [Eq. (1)] of about 300 nm with  $D$  estimated from thermal conductivity, density, and specific heat values.<sup>11,90</sup> Therefore, only the near surface region of the  $\text{CI(G)Se}$  film is affected by the laser energy, with the film bulk remaining unaltered (see Fig. 3). As a result of  $l_t$  being much less than the film thickness, the bulk of the film must already show suitable characteristics for a device prior to annealing, therefore, these studies use only “high” quality  $\text{CISE/CIGSe}$  absorbers, formed using either method (1) single step co-evaporation, or a precursor formed using method (2) that has been thermally treated prior to LA.

The unsuitability of PLA for absorber formation is exemplified in the work of Bhatia et al., who carried out PLA on similar electrodeposited  $\text{CISE}$  precursors to those which were successfully CW LA using a 1064-nm Nd:YAG laser. While both the Nd:YAG laser in pulsed mode (pulse time 75 to 150 ns) and a 248 nm KrF laser ( $\approx 25 \text{ ns}$ ) induced some crystal growth at high flux, they also caused the  $\text{CISE}$  to melt and dewet.<sup>81,91,92</sup> PLA in the sub-melting regime ( $\leq 70 \text{ mJ cm}^{-2}$ ) had no measurable effect on the structural properties of the  $\text{CISE}$  film. As this fluence exceeded that which was later shown to produce both structural and optoelectronic improvements in high quality  $\text{CISE}$  absorbers, it is concluded that this result is due to the poor thermal transport in the nanocrystalline and multiphase, as-deposited  $\text{CISE}$  precursors.<sup>83</sup> Only by melting the film is a sufficient atomic mobility and energy available for  $\text{CISE}$  formation throughout its full thickness. As the dewetting of the liquid phase  $\text{CISE}$  occurs spontaneously on all

tested substrates,<sup>67</sup> it was concluded that there is no practical processing window that allows PLA to be used for CIGSe absorber formation.

The first published studies of sub-melt PLA of CIGSe were carried out by the group of Anderson,<sup>93–95</sup> which used co-evaporated Cu(In,Ga)Se<sub>2</sub> absorbers as pictured in Fig. 7b(i) with a CdS buffer layer deposited on the surface. Having identified that interfacial recombination at the CIGSe/CdS interface is a limiting factor to optimal device performance the authors used PLA to modify near-surface defects in the CIGSe absorber. Initially, they tested the effect of five pulses with energy densities from 20 to 60 mJ cm<sup>-2</sup>. XRD showed a slight increase in crystallographic order compared to the un-irradiated film, indicating that the laser energy is sufficient to stimulate atomic diffusion. All conditions were shown by dual beam optical modulation to increase the charge carrier lifetime, with the lowest fluence giving the most significant improvement with a near tripling of this value. Furthermore, Hall measurements showed an increase in carrier mobility and decrease in film resistance. Both of these results are consistent with PLA removing near-surface electrically active defect states. As these states act as carrier traps and recombination centers, it was expected that PLA should lead to devices with higher efficiencies. However, devices formed from samples irradiated at 50 mJ cm<sup>-2</sup> showed equivalent efficiencies to the un-irradiated control. This was explained using external quantum efficiency measurements, which showed a decrease in carrier collection at wavelengths <630 nm after laser irradiation. This indicated that the poor device performance could be due to the laser pulse also causing damage in the CIGSe/CdS interface region. Increasing the pulse number to 10 or 20 pulses<sup>93</sup> also showed similar improvements in Hall mobility. However, device measurements revealed that only the lowest laser fluence (30 mJ cm<sup>-2</sup>) led to an efficiency increase over the 9.1% efficient reference device. Fluences of 40 mJ cm<sup>-2</sup> or higher degraded the cell performance, consistent with increased laser damage. Measurements of the low-fluence annealed devices yielded 12.1% and 11.1% efficiencies for 5 and 10 pulses, respectively. Although not a recorded result, it does show a remarkable 33% relative improvement with a process that takes less than 1 s to perform.

Ahmed et al. carried out a detailed analysis of the defect energy levels in CIGSe films formed using flash evaporation.<sup>96</sup> The slight increase in bandgap from 1.00 to 1.02 after five pulses ( $w \approx 20$  ns time) of laser irradiation at 170 mJ was claimed to be related to a modification of defect levels at the band edge. High-resolution photoacoustic spectroscopy revealed the ionization and proposed electrical activities of five deep-level defects, which provide non-radiative recombination pathways within the film. However, upon close scrutiny, it is clear that these purported defect absorption transitions correspond to the narrow peaks in the illuminating lamp's spectrum. It is well known that it is difficult to normalize such spectra, and it is common to see artifact peaks arising from imperfect normalization. Also, defect-to-band transitions, which should be more probable than discrete defect-to-defect transitions, will produce an onset in absorption and not a resonant peak. We conclude that it is possible that some changes in sub-bandgap absorption were responsible for the observed changes in photoacoustic absorption; however, the data are rife with experimental artifacts so the conclusions should be carefully examined. The position and intensity of near-edge absorption features were claimed to become less pronounced with LA but with an additional consequence of forming a shallow defect near the band edge.

Bhatia et al. measured the PL yield after LA of co-electrodeposited CIGSe samples with five pulses of fluences from 20 to 40 mJ cm<sup>-2</sup>.<sup>91,97</sup> Current-voltage curves measured in the dark showed an improvement in the diode ideality factor at fluences of 20 and 30 mJ cm<sup>-2</sup>.<sup>97</sup> The increased PL yield with LA was attributed to an increase in radiative transitions due to a reduction in deep-defect concentration. However, an observed PL broadening was indicative of a more highly compensated semiconductor, which can be caused by an increased concentration of shallow defects. Deep-level transient spectroscopy and temperature-dependent admittance spectroscopy indicated that this shallow trap state was around 60 meV and detected the presence of a majority hole trap at 200 meV. The formation of shallow defects may be due to laser processing in an inert atmosphere. A low Se activity during annealing has been shown to lead to formation of V<sub>Se</sub> and the shallow defect In<sub>Cu</sub>, both of which are detrimental to device performance.<sup>87</sup> This assumption is further supported by Ref. 98 where the Schottky barrier height for the CIGSe film annealed at the highest fluence indicated the presence of oxide phases and/or a high density of interface states, possibly from Se vacancies.

In this section, it has been shown that pulsed, non-melted LA has the potential to improve the structural and optoelectronic characteristics of chalcogenide absorber layers. By reducing the deep-level defects, particularly those localized at the film surface, a material with an improved carrier lifetime is achieved. This has the potential to increase the short circuit current,  $J_{SC}$ , of the final devices fabricated from these films, and therefore, increase device efficiency. However, a counter effect of the technique appears to be the creation of shallow defects and surface damage with higher fluences. Consequently, there is only a narrow processing window for PLA of CI(G) Se, in which the potential of this processing step is realized.

## 4 Summary and Conclusions

LA, both CW and pulsed, is amenable to achieving many properties desired in high-quality, thin film chalcogenide-based solar cells. This review details our own and the body of published work that has been performed in this area and also identifies areas for further research on the utilization of lasers for applications aside from scribing in thin film solar cell production. Specific to CdTe solar cells, the ability to address major technological issues such as Ohmic contact formation and cost reduction through low-cost and rapid processing has all been demonstrated, to varying degrees, with laser processes. A rapid succession of nanosecond laser pulses has successfully altered the surface stoichiometry to make a Te-rich surface to facilitate an Ohmic back contact to CdTe. Furthermore, CW processes have been explored for both rapid thin film formation from low-cost precursors as well as defect annealing and recrystallization. We have ongoing efforts in this area which are yielding exciting preliminary results.

Similarly, themed research efforts have also been undertaken for CI(G)Se-based solar cells. CW annealing has been shown to reduce annealing times required for absorber formation from precursors by orders of magnitude compared to current processes. The potential of LA in a CI(G) Se fabrication method has been demonstrated by a prototype device, and clear steps for process optimization of increasing beam homogeneity and Se activity have been identified. Industrially implementing such a process would increase throughput and potentially reduce capital expenditures of absorber layer production. Pulsed lasers have been shown to increase relative device efficiency by more than 30% with the application of only a few nanosecond pulses. This was achieved by surface defect modification thought to be limiting  $J_{SC}$  through surface recombination. The relative ease with which this remarkable result was achieved highlights the potential of using PLA in solar cell device manufacturing. These results provide evidence of the value of a laser processing step in CIS/CIGSe absorber fabrication. It remains to be seen, however, if such benefits can be realized on materials and devices already demonstrating near-record efficiency.

## Acknowledgments

The work at University of Utah and University of South Florida on CdTe was supported in full by the Department of Energy via the Bay Area Photovoltaic Consortium under prime award DE-EE0004946. The work at the University of Utah on CuInSe<sub>2</sub> was supported in full by the National Science Foundation Materials World Network program award 1008302. B.S. and M.S. would like to thank Dr. Naba Paudel at the University of Toledo for the sputtered CdTe films. H.M. and P.D. acknowledge the Fonds National de la Recherche du Luxembourg for grant MAT09/02 and AFR grant RASER and David Regesch and Maxime Thevenin for the PL and SEM measurements respectively.

## References

1. A. Hauser et al., "Comparison of different techniques for edge isolation," in *Proc. 17th Eur. Photovolt. Sol. Energy Conf.*, pp. 1739–1741, ETA-Florence, Italy (2001).
2. D. Kyeong et al., "Laser edge isolation for high-efficiency crystalline silicon solar cells," *J. Korean Phys. Soc.* **55**(1), 124–128 (2009).
3. J. M. Gee, W. K. Schubert, and P. A. Basore, "Emitter wrap-through solar cell," in *23rd IEEE Photovolt. Spec. Conf.*, p. 265, IEEE (1993).

4. J. C. Zolper et al., "16.7% efficient, laser textured, buried contact polycrystalline silicon solar cell," *Appl. Phys. Lett.* **55**(22), 2363–2365 (1989).
5. E. Schneiderloechner et al., "Laser-fired rear contacts for crystalline silicon solar cells," *Prog. Photovoltaics Res. Appl.* **10**(1), 29–34 (2002).
6. L. Wang, D. E. Carlson, and M. C. Gupta, "Silicon solar cells based on all-laser-transferred contacts," *Prog. Photovoltaics Res. Appl.* (2013).<http://onlinelibrary.wiley.com/doi/10.1002/pip.2395/abstract>
7. D. E. Carlson, "Laser processing of solar cells," *Proc. SPIE* **8473**, 847302 (2012).
8. C. M. Dunskey, "The promise of solar energy: applications and opportunities for laser processing in the manufacturing of solar cells," *Proc. SPIE* **6459**, 64590 (2007).
9. M. Pinarbasi et al., "Flexible cells and modules produced using roll-to-roll electroplating approach," in *2010 35th IEEE Photovolt. Spec. Conf.*, pp. 169–174, IEEE, Honolulu, Hawaii (2010).
10. J. Dore et al., "Progress in laser-crystallized thin-film polycrystalline silicon solar cells: intermediate layers, light trapping, and metallization," *IEEE J. Photovoltaics* **4**(1), 33–39 (2014).
11. A. D. Compaan, I. Matulionis, and S. Nakade, "Laser scribing of polycrystalline thin films," *Opt. Lasers Eng.* **34**(1), 15–45 (2000).
12. R. Murison et al., "CIGS P1, P2, P3 scribing processes using a pulse programmable industrial fiber laser," in *Proc. 35th IEEE PVSC*, pp. 179–184, IEEE (2010).
13. A. Chirila et al., "Highly efficient Cu(In, Ga)Se<sub>2</sub> solar cells grown on polymer films," *Nat. Mater.* **10**, 857–861 (2011).
14. J. Perrenoud et al., "Fabrication of flexible CdTe solar modules with monolithic cell integration," *Sol. Energy Mater. Sol. Cells* **95**, S8–S12 (2011).
15. C. Uzan et al., "CW laser induced low-temperature decomposition of CdTe crystals," *Appl. Phys. Lett.* **45**(8), 879 (1984).
16. R. O. Bell, M. Toulemonde, and P. Siffert, "Calculated temperature distribution during laser annealing in silicon and cadmium telluride," *Appl. Phys.* **19**, 313–319 (1979).
17. B. J. Simonds et al., "Sub-bandgap laser annealing of room temperature deposited polycrystalline CdTe," *Proc. SPIE* **9180**, 91800F (2014).
18. B. J. Simonds et al., "Pulsed UV laser annealing of polycrystalline CdTe," *Proc. SPIE* **8826**, 882607 (2013).
19. J. M. Poate and J. W. Mayer, Eds., *Laser Annealing of Semiconductors*, Academic Press, Inc., New York (1982).
20. J. J. Alvarado et al., "Thermal properties of CdTe," *J. Appl. Phys.* **76**(11), 7217 (1994).
21. "First Solar, Inc. Announces Fourth Quarter and Full Year 2013 Financial Results," 2014, <http://investor.firstsolar.com/releasedetail.cfm?ReleaseID=825848> (18 December 2014).
22. "First Solar Sets World Record for CdTe Solar Cell Efficiency," 2014, <http://investor.firstsolar.com/releasedetail.cfm?ReleaseID=828273> (18 December 2014).
23. ZSW, "ZSW Brings World Record Back to Stuttgart," 2014, <http://www.zsw-bw.de/uploads/media/pr12-2014-ZSW-WorldrecordCIGS.pdf> (18 December 2014).
24. "Research Cell Efficiency Record," [http://www.nrel.gov/ncpv/images/efficiency\\_chart.jpg](http://www.nrel.gov/ncpv/images/efficiency_chart.jpg) accessed (6 August 2014).
25. S. H. Demtsu and J. R. Sites, "Effect of back-contact barrier on thin-film CdTe solar cells," *Thin Solid Films* **510**(1–2), 320–324 (2006).
26. D. Kraft et al., "Alternative back contacts for CdTe solar cells: a photoemission study of VSe<sub>2</sub>/CdTe and TiSe<sub>2</sub>/CdTe interface formation," *Thin Solid Films* **431–432**, 382–386 (2003).
27. G. Stollwerck and J. R. Sites, "Analysis of CdTe back-contact barriers," in *Proc. 13th European Photovoltaics Solar Energy Conf.*, pp. 2020–2022 (1995) <https://www.photovoltic-conference.com/conference/conference-proceedings.html>.
28. B. J. Simonds et al., "Pulsed laser induced ohmic back contact in CdTe solar cells," *Appl. Phys. Lett.* **104**, 141604 (2014).
29. J. M. Frey, "Modified cadmium telluride layer, a method of modifying a cadmium telluride layer, and a thin film device having a cadmium telluride layer," US20110308593 A1, USA (2010).

30. A. Baidullaeva et al., "CdTe polycrystalline surface subjected to pulsed laser irradiation," *Semiconductors* **35**(6), 745–748 (2001).
31. P. D. Brewer, J. J. Zinck, and G. L. Olson, "Reversible modification of CdTe surface composition by excimer laser irradiation," *Appl. Phys. Lett.* **57**(24), 2526 (1990).
32. B. J. Simonds et al., "Surface stoichiometry of pulsed ultraviolet laser treated polycrystalline CdTe surface stoichiometry of pulsed ultraviolet laser treated polycrystalline CdTe," *J. Appl. Phys.* **116**, 013506 (2014).
33. D. W. Niles et al., "Evaporated Te on CdTe: a vacuum-compatible approach to making back contact to CdTe solar cell devices," *Prog. Photovoltaics Res. Appl.* **4**, 225–229 (1996).
34. D. Kraft et al., "Characterization of tellurium layers for back contact formation on close to technology treated CdTe surfaces," *J. Appl. Phys.* **94**(5), 3589 (2003).
35. V. Montgomery and J. H. Dinana, "Characteristics of CdTe surfaces prepared by pulsed laser irradiation," *Thin Solid Films* **124**(1), 11–17 (1985).
36. L. A. Golovan et al., "Investigation of laser-induced defect formation in CdTe crystals by Rutherford backscattering," *Phys. Solid State* **40**(2), 187–189 (1998).
37. V. A. Gnatyuk, "Characterization of laser-irradiated CdxHg1-xTe solid solutions by scanning microscopy method," *Solid State Phenom.* **63–64**, 353–360 (1998).
38. V. A. Gnatyuk et al., "Surface state of CdTe crystals irradiated by KrF excimer laser pulses near the melting threshold," *Surf. Sci.* **542**(1–2), 142–149 (2003).
39. L. A. Golovan et al., "Evaporation effect on laser induced solid-liquid phase transitions in CdTe and HgCdTe," *Solid State Commun.* **108**(10), 707–712 (1998).
40. A. J. Nelson et al., "Scanning photoelectron microscopy study of the laser-induced transformations of polycrystalline CdTe films," *J. Appl. Phys.* **87**(7), 3520 (2000).
41. C. Arnone, M. Rothschild, and D. J. Ehrlich, "Laser etching of 0.4  $\mu\text{m}$  structures in CdTe by dynamic light guiding," *Appl. Phys. Lett.* **48**(11), 736 (1986).
42. M. Rothschild, C. Arnone, and D. J. Ehrlich, "Laser photosublimation of compound semiconductors," *J. Mater. Res.* **2**(2), 244–251 (1987).
43. S. Sugai, "Photoinduced tellurium precipitation in CdTe," *Jpn. J. Appl. Phys.* **30**(Part 2, No. 6B), 1083–1085 (1991).
44. M. J. Soares, "Raman characterization of Te inclusions on CdTe surface using visible lasers," *Proc. SPIE* **4469**, 57–61 (2001).
45. M. J. Soares et al., "Micro-Raman study of laser damage in CdTe," *Phys. Status Solidi* **1**(2), 278–280 (2004).
46. P. M. Amirtharaj and F. H. Pollak, "Raman scattering study of the properties and removal of excess Te on CdTe surfaces," *Appl. Phys. Lett.* **45**(7), 789 (1984).
47. D. I. Tsyutsyura and P. S. Shkumbatyuk, "Fabrication of p-n junctions from CdTe:In by laser annealing," *Semiconductors* **27**(6), 579–580 (1993).
48. C. A. Wolden et al., "Photovoltaic manufacturing: Present status, future prospects, and research needs," *J. Vac. Sci. Technol. A* **29**(3), 030801 (2011).
49. M. Woodhouse et al., "The present, mid-term, and long-term supply curves for tellurium; and updates in the results from NREL's CdTe PV module manufacturing cost model," NREL/PR-6A20-60430, Golden, Colorado (2013).
50. Y. Ma et al., "Preparation of CdTe nanostructures with different crystal structures and morphologies," *Powder Diffr.* **26**(S1), S47–S50 (2011).
51. Y. Yan et al., "Observation and first-principles calculation of buried wurtzite phases in zincblende CdTe thin films," *Appl. Phys. Lett.* **77**(10), 1461 (2000).
52. A. L. Dawar et al., "Effect of laser annealing on the structural, electrical, and optical properties of CdTe thin films," *Appl. Surf. Sci.* **22/23**, 846–858 (1985).
53. N.-H. Kim, C. I. Park, and J. Park, "A pilot investigation on laser annealing for thin-film solar cells: crystallinity and optical properties of laser-annealed CdTe thin films by using an 808-nm diode laser," *J. Korean Phys. Soc.* **62**(3), 502–507 (2013).
54. D. J. As and L. Palmetshofer, "Laser annealing of defects in CdTe epitaxial layers," *J. Cryst. Growth* **72**, 246–251 (1985).
55. N. V. Sochinskii et al., "Laser-assisted recrystallization to improve the surface morphology of CdTe epitaxial layers," *Semicond. Sci. Technol.* **11**(2), 248–251 (1996).

56. FC. B. Norris and P. S. Peercy, "Defect reactions and effect of coimplants and prior heat treatment in pulsed laser annealing of ion-implanted CdTe:In and CdTe:Cl," *Radiat. Eff.* **69**, 267–275 (2006).
57. C. Uzan, R. Legros, and Y. Marfaing, "A comparative study of laser and furnace annealing of P+ implanted CdTe," *J. Cryst. Growth* **72**, 252–257 (1985).
58. P. Bhattacharya et al., "Laser annealing of phosphorus-implanted CdTe," *Mater. Sci. Eng.* **B5**, L1–L3 (1990).
59. J. Schuller et al., "Thermal and laser annealing of intrinsic defects in CdTe epilayers," in *Proc. 13th Int. Conf. Defects Semicond.*, pp. 553–559 (1984) <http://www.worldcat.org/title/proceedings-of-the-13th-international-conference-on-defects-in-semiconductors-held-at-coronado-california-august-12-17-1984/oclc/82447487>.
60. L. Baufay et al., "Laser induced formation of CdTexSe1-x semiconducting compounds," *J. Cryst. Growth* **59**, 143–147 (1982).
61. P. C. Pande et al., "Recrystallisation of electrophoretically deposited CdTe films," *J. Cryst. Growth* **159**, 930–934 (1996).
62. J. J. Zinck et al., "Excimer laser-assisted metalorganic vapor phase epitaxy of CdTe on GaAs," *Appl. Phys. Lett.* **52**(17), 1434 (1988).
63. C. D. Stinespring and A. Freedman, "Laser induced surface chemical epitaxy," *Proc. SPIE* **1190**, 35–40 (1990).
64. K. M. Rickey et al., "Effects of rapid thermal processing and pulse-laser sintering on CdTe nanofilms for photovoltaic applications," *Proc. SPIE* **8465**, 846505 (2012).
65. D. Berg, "Kesterite equilibrium reaction and the discrimination of secondary phases from Cu<sub>2</sub>ZnSnS<sub>4</sub>," Thesis, Universite du Luxembourg (2012).
66. Z.-H. Li et al., "Formation of CuInSe<sub>2</sub> absorber by rapid thermal processing of electron-beam evaporated stacked elemental layers," *J. Mater. Sci. Mater. Electron.* **23**(4), 964–971 (2012).
67. A. Bhatia et al., "Continuous wave solid phase laser annealing of single-pot electrodeposited CuInSe<sub>2</sub> thin films: effects of Cu/In stoichiometry," *J. Appl. Phys.* **114**(4), 044904 (2013).
68. L. D. Laude, M. C. Joliet, and C. Antoniadis, "Laser-induced synthesis of thin CuInSe<sub>2</sub> films," *Sol. Cells* **16**, 199–209 (1986).
69. M. C. Joliet et al., "Laser-induced synthesis of thin CuInSe<sub>2</sub> films," *Appl. Phys. Lett.* **46**(3), 266–267 (1985).
70. D. Bhattacharyya, S. Bocking, and M. J. Carter, "Detection of binary phases in CuInSe<sub>2</sub> films formed by laser annealing of stacked elemental layers of In, Cu and Se," *J. Mater. Sci.* **31**(20), 5451–5456 (1996).
71. R. Scheer and H.-W. Schock, *Chalcogenide Photovoltaics: Physics, Technologies, and Thin Film Devices*, Wiley-VCH Verlag GmbH & Co, Weinheim, Germany (2011).
72. M. Wakaki, K. Kudo, and T. Shibuya, *Physical Properties and Data of Optical Materials*, CRC Press, Taylor and Francis Group, Boca Raton, Florida (2007).
73. T. Tinoco et al., "Phase diagram and optical energy gaps for CuInyGa1-ySe<sub>2</sub> Alloys," *Phys. Status Solidi* **124**(2), 427–434 (1991).
74. T. Walter, M. J. Carter, and R. Hill, "Laser induced synthesis of copper indium diselenide for solar applications," in *Proc. 9th Eur. Photovoltaic Sol. Energy Conf.*, Freiburg, Germany (1989).
75. S. Jost et al., "The formation of CuInSe<sub>2</sub> thin-film solar cell absorbers by laser annealing of electrodeposited precursors," *Sol. Energy Mater. Sol. Cells* **92**(4), 410–417 (2008).
76. B. J. Stanbery, "Copper indium selenides and related materials for photovoltaic devices," *Crit. Rev. Solid State Mater. Sci.* **27**(2), 73–117 (2002).
77. S. R. Kodigala, *Cu(In1-xGax)Se2 Based Thin Film Solar Cells*, Academic Press, Inc., Burlington, Massachusetts (2011).
78. P. Jackson et al., "New world record efficiency for Cu(In, Ga)Se<sub>2</sub> thin-film solar cells beyond 20%," *Prog. Photovoltaics Res. Appl.* **19**, 894–897 (2011).
79. V. Deprédurand et al., "Current loss due to recombination in Cu-rich CuInSe<sub>2</sub> solar cells," *J. Appl. Phys.* **115**(4), 044503 (2014).
80. G. D. Mooney and A. M. Hermann, *Novel Thin-Film CuInSe<sub>2</sub> Fabrication*, Solar Energy Research Institute, Golden, Colorado (1989).

81. A. Bhatia et al., "Pulsed and continuous wave solid phase laser annealing of electrodeposited CuInSe<sub>2</sub> thin films," *Proc. SPIE* **8473**, 84730F (2012).
82. A. Ashour, "Some physical properties of CuInSe<sub>2</sub> thin films," *J. Mater. Sci. Mater. Electron.* **17**(8), 625–629 (2006).
83. H. J. Meadows et al., "Single second laser annealed CuInSe<sub>2</sub> semiconductors from electrodeposited precursors as absorber layers for solar cells," *J. Phys. Chem. C* **118**(3), 1451–1460 (2014).
84. H. J. Meadows et al., "Crystallographic study of phases present in CuInSe<sub>2</sub> absorber layers produced by laser annealing co-electrodeposited precursors," *Proc. SPIE* **8823**, 882302 (2013).
85. H. J. Meadows et al., "CuInSe<sub>2</sub> semiconductor formation by laser annealing," *Thin Solid Films*, in press (2014) <http://www.sciencedirect.com/science/article/pii/S0040609014010037>.
86. H. J. Meadows et al., "The importance of Se partial pressure in the laser annealing of CuInSe<sub>2</sub> electrodeposited precursors," in *Proc. 40th IEEE PVSC*, pp 405–408, IEEE (2014).
87. Q. Cao et al., "Defects in Cu(In, Ga)Se<sub>2</sub> chalcophyrite semiconductors: a comparative study of material properties, defect states, and photovoltaic performance," *Adv. Energy Mater.* **1**(5), 845–853 (2011).
88. H. J. Meadows et al., "Photovoltaic devices produced from electrodeposited CuInSe<sub>2</sub> precursors using 1 s laser annealing," *Prog. Photovoltaics Res. Appl.*, in press (2014).
89. J. M. Poate, P. S. Peercy, and S. U. Campisano, "Laser annealing of Si," in *Laser Surface Treatment of Metals*, p. 595, C. W. Draper and P. Mazzoldi, Eds., Martinus Nijhoff, Dordrecht (1986).
90. T. Tinoco et al., "Structural studies of CuInS<sub>2</sub> and CuInSe<sub>2</sub> under high pressure," *Phys. Status Solidi* **198**(1), 433–438 (1996).
91. A. Bhatia et al., "Pulsed laser processing of electrodeposited CuInSe<sub>2</sub> photovoltaic absorber thin films," in *Proc. 37th IEEE PVSC*, pp. 329–332, IEEE (2011).
92. A. Bhatia et al., "Pulsed laser processing of electrodeposited CuInSe<sub>2</sub> photovoltaic absorber thin films," in *MRS Proceedings*, Vol. 1268, pp. 1268–EE04–10 (2010).
93. T. J. Anderson et al., "Fundamental materials research subcontract and advanced process development for thin-film CIS-based photovoltaics," Subcontract Report, NREL/SR-520-40568 (2006).
94. X. Wang et al., "Investigation of pulsed non-melt laser annealing (NLA) of CIGS-based solar cells," in *Proc. 3rd World Conf. Photovolt. Energy Convers.*, pp. 396–399, IEEE (2003).
95. X. Wang et al., "Investigation of pulsed laser annealing (PLA) and rapid thermal annealing (RTA) of CIGS films and solar cell," in *Conf. Rec. Thirty-first IEEE Photovolt. Spec. Conf.*, pp. 394–397, IEEE (2005).
96. E. Ahmed et al., "Laser annealing of flash-evaporated CuInSe<sub>2</sub> thin films," *J. Mater. Eng. Perform.* **15**, 213–217 (2006).
97. A. Bhatia et al., "Study of point defects in ns pulsed-laser annealed CuInSe<sub>2</sub> thin films," in *Conf. Rec. 38th IEEE Photovolt. Spec. Conf.*, pp. 1–5 (2012) [http://ieeexplore.ieee.org/xpl/login.jsp?tp=&arnumber=6656702&url=http%3A%2F%2Fieeexplore.ieee.org%2Fxppls%2Fabs\\_all.jsp%3Farnumber%3D6656702](http://ieeexplore.ieee.org/xpl/login.jsp?tp=&arnumber=6656702&url=http%3A%2F%2Fieeexplore.ieee.org%2Fxppls%2Fabs_all.jsp%3Farnumber%3D6656702).
98. A. Bhatia et al., "Effects of pulsed laser annealing on deep level defects in electrochemically-deposited and furnace annealed CuInSe<sub>2</sub> thin films," *Thin Solid Films* **531**, 566–571 (2013).

**Brian J. Simonds** is currently a research associate at the University of Colorado Boulder and the National Institute of Standards and Technology. He has a BSc in physics from Illinois Wesleyan University and a PhD in applied physics from Colorado School of Mines. He pursued postdoctoral research at the University of Utah, investigating laser processing of thin film photovoltaic materials. His research interests include advanced laser/material phenomenon and photovoltaic material processing.

**Helene J. Meadows** is currently completing her PhD in physics at the University of Luxembourg on the laser annealing of Cu(In, Ga)Se<sub>2</sub> as absorber layers for thin film solar cells. Prior to her PhD, she earned a master's degree in chemistry from the University of

Bath, UK, during which she undertook a year in industry working as an intern for the Dutch polymer manufacturer DSM in Geleen, Netherlands. Her interests lie in sustainable energy and development.

**Sudhajit Misra** received his bachelor's degree in technology from Biju Patnaik University of Technology, India, in 2010. He is currently pursuing a PhD working with Dr. Mike Scarpulla in the Department of Electrical and Computer Engineering, University of Utah. Prior to starting his graduate studies, he was working as an engineer at Vedanta Aluminium Ltd., India. His research focuses on laser processing and characterization of CdTe for thin film photovoltaic applications.

**Christos Ferekides** is a professor of electrical engineering at the University of South Florida. He received his PhDEE degree from USF. His research focuses on opto-electronic applications with emphasis on the growth and characterization of photovoltaic materials and devices. He has authored/co-authored over 60 publications.

**Phillip J. Dale** is a senior lecturer in the physics and materials science research unit of the University of Luxembourg. He received both his master's degree in chemistry and his PhD in colloid science from the University of Bristol. His career focuses on the growth and characterization of thin film II-VI semiconductors using low energy methods, with particular attention to earth abundant materials. He has (co) authored over 50 publications, four book chapters, and holds two patents.

**Michael A. Scarpulla** is an associate professor in the Departments of Materials Science & Engineering and Electrical & Computer Engineering at the University of Utah and is an editor for the *IEEE Journal of Photovoltaics*. In 2000, he earned an ScB from Brown University and in 2006 earned a PhD from UC Berkeley, both in MSE. Prior to joining Utah in 2008, he was a postdoctoral researcher at UC Santa Barbara. His research focuses on laser processing and advanced characterization of semiconductors primarily for thin film photovoltaics.